A matrix converter based Inductive Power Transfer system

Nguyen Xuan Bac, D. Mahinda Vilathgamuwa
School of Electrical and Electronics Engineering
Nanyang Technological University, Singapore
Email: xuanbac001@e.ntu.edu.sg; emahinda@ntu.edu.sg

Udaya K. Madawala
Department of Electrical & Computer Engineering
University of Auckland, New Zealand
Email: u.madawala@auckland.ac.nz

***Abstract*—Typical Inductive Power Transfer (IPT) systems employ two power conversion stages to generate a high frequency current from low frequency utility supply. This paper proposes a matrix converter based IPT system that facilitates the generation of high frequency current through a single power conversion stage. The proposed matrix converter topology transforms a 3-phase low frequency voltage system to a high frequency single phase voltage which in turn powers a series compensated IPT system. A comprehensive mathematical model is developed to investigate the behavior of the proposed IPT topology. Theoretical results are presented in comparison to simulations, which are performed in Matlab/ Simulink, to demonstrate the applicability of the proposed concept and the validity of the developed model.**

Keywords: matrix converter, inductive power transfer, IPT.

I. INTRODUCTION

Inductive Power Transfer systems are gaining popularity as they offer numerous advantages over conventional wired power transfer systems in relation to convenience, safety, isolation, operation in hostile conditions and flexibility. Consequently, there is an increased demand for IPT powered applications, such as transportation [1]-[2], mobile devices charging, lighting, material handling, mobile control robots [4]-[6], bio-medical implants [7], etc.

Development of efficient IPT systems can be considered as receiving more attention as many attempts have recently been made to improve the overall efficiency. The overall efficiency of an IPT system largely depends on the losses that incur in coupling coils and converters. In case of the former, the losses can be minimized by proper magnetic circuit and coil winding design, whereas in the later, with the reduction of number of conversion stages, switching and conduction losses can be reduced.

A typical IPT system is shown in Fig. 1. The primary side comprises an AC source, a rectifier, an inverter and a resonant network to compensate the primary coil inductance. The secondary, mutually coupled to the primary through M, employs a resonant compensation network and a power regulator, which can be a rectifier in the simplest form. As evident, two power conversion stages are invariably required on the primary side to generate a high frequency current in the primary coil. In addition a DC-link capacitor is also used to reduce the voltage ripple. Consequently, the system suffers from disadvantages such as lower reliability, increase in power losses, cost and overall physical size.

A matrix converter can be employed to reduce the number of conversion stages and, thereby, to alleviate some of the above disadvantages. A single stage AC to AC conversion through a matrix converter has been proposed by Venturini and Alesina in 1980's and since became popular as an alternative to conventional indirect power converter systems [8]. The matrix converter concept facilitates the synthesis of a high frequency voltage or current directly from a low frequency supply source, and is ideal for generating a high frequency current, which is required for IPT systems, directly from the supply mains.

This paper proposes a matrix converter based IPT system that generates a high frequency current with a reduced number of semiconductor switches. The proposed topology transforms 50-Hz 3-phase utility supply to a single-phase high frequency supply which in turn can be used to directly excite the primary side resonant network of an IPT system [9]-[11]. Fig. 2 shows the IPT system, driven by the proposed matrix converter based topology. Series compensation is provided for both sides of the IPT system.

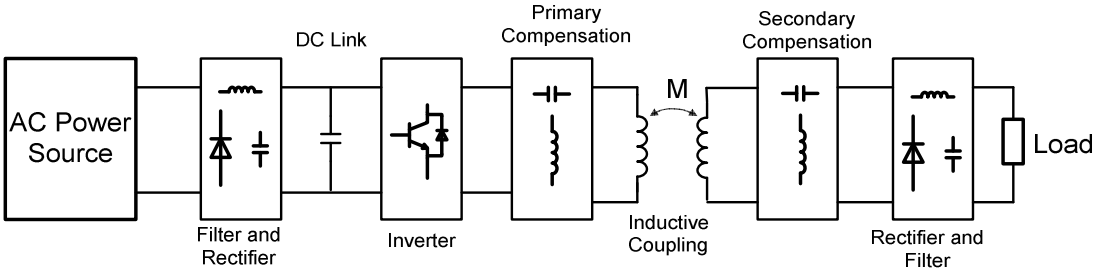

Fig. 1. A typical IPT system with AC power supply

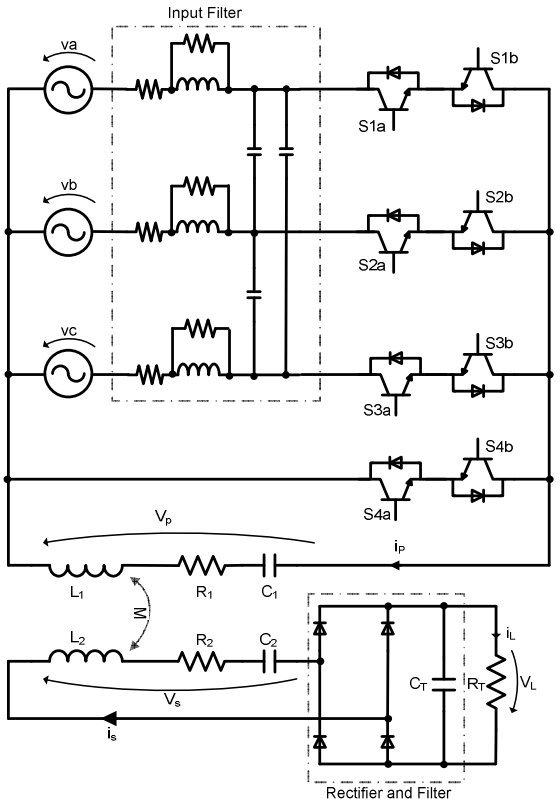

Fig. 2. IPT system with the proposed matrix converter topology.

II. THREE PHASE TO SINGLE PHASE MATRIX CONVERTER COMMUTATION STRATEGY

A. The proposed matrix converter and commutation strategy

In the proposed topology, a three-phase to single-phase matrix converter with only 4 bi-directional switches is employed to produce a high frequency current in the primary side series resonant tank. The fourth switch is added to control the resonant energy through a zero-voltage state across the resonant tank or V_p. The switching strategy is described in Fig. 3.

The basic switching rule is that only one bi-directional switch is switched on at any instant. The basic 4-step commutation is employed in this case. So the output voltage will be either equal to zero, or equals to one of three phase voltages. In case the output voltage is equal to the phase voltage, it should be switched to the phase which is the boundary of three phase voltage as shown in Fig. 3(a), i.e. maximum voltage v^+ or minimum voltage v^-. The zero voltage state is controlled by switching on *S4*.

By using the phase shift control method [1]-[3], the output voltage will have the waveform illustrated in Fig. 3(f).

To analyze the fundamental component and higher order harmonics of output voltage v_p, let us define v^+, v^-, f^+ and f^- as shown in Fig. 3.

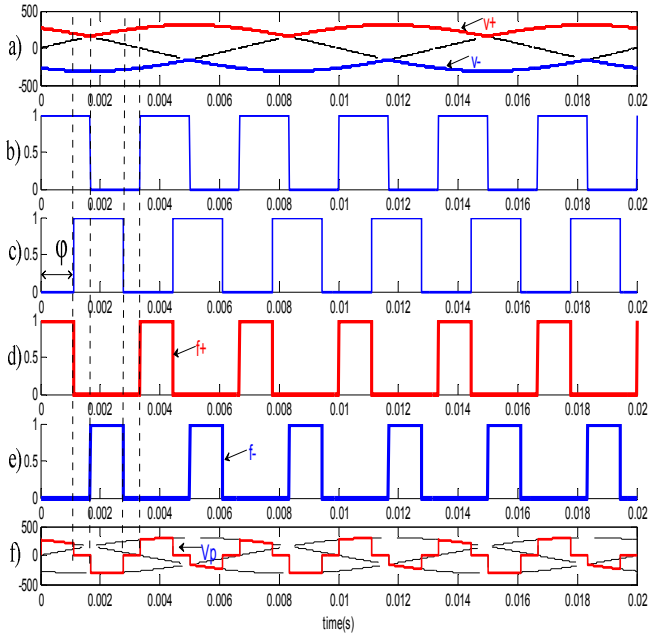

Fig. 3. Commutation strategy with phase shift control method, (a) three phase input voltage with boundary voltages highlighted, (b), (c) phase shift control signals, (d), (e) positive and negative side control signals, (f) primary voltage of resonant load.

B. Steady-State Harmonic Analysis

Assume that the three phase input voltages are given as follows

$$\begin{aligned} v_a(\omega_0 t) &= V_m \sin(\omega_0 t) \\ v_b(\omega_0 t) &= V_m \sin(\omega_0 t - \frac{2\pi}{3}) \\ v_c(\omega_0 t) &= V_m \sin(\omega_0 t + \frac{2\pi}{3}) \end{aligned} \tag{1}$$

with ω_0 is the AC input voltage angular frequency and V_m is the amplitude of input phase voltages.

The positive and negative components of boundary input voltage is respectively given by

$$v^+(\omega_0 t) = \begin{cases} V_m \sin(\omega_0 t) & \frac{\pi}{6} \le \omega_0 t \le \frac{5\pi}{6} \\ v^+(\omega_0 t + \frac{k2\pi}{3}) & , otherwise; (k \in \mathbb{Z}) \end{cases} \tag{2}$$

and

$$v^-(\omega_0 t) = -v^+(\omega_0 t + \frac{2\pi}{3}) \tag{3}$$

And using Fourier expansion,

$$v^+(t) = \frac{3\sqrt{3}V_m}{2\pi}\left[1 - \sum_{n=1}^{+\infty} \frac{2}{9n^2 - 1}\cos(3n\omega_0 t - \frac{n\pi}{2})\right] \tag{4}$$

and

$$v^{-}(t)=-\frac{3\sqrt{3}V_m}{2\pi}\left[1-\sum_{n=1}^{+\infty}\frac{2*(-1)^n}{9n^2-1}\cos(3n\omega_0 t-\frac{n\pi}{2})\right] \quad (5)$$

Let us define the frequency of square wave for phase shift method be f_T. f_T therefore is also the resonant frequency in both primary and pick up side of IPT system. So the resonant angular frequency will be

$$\omega_T=2\pi f_T=\frac{1}{\sqrt{L_1C_1}}=\frac{1}{\sqrt{L_2C_2}} \quad (6)$$

The phase shift pulse patterns f^{+} and f^{-} as seen in Fig. 3(d) and Fig. 3(e) are respectively given by

$$f^{+}(t)=\frac{\varphi}{2\pi}+\sum_{n=1}^{+\infty}\left[\frac{2}{n\pi}\cos(n\omega_T t-\frac{n\varphi}{2})\sin(\frac{n\varphi}{2})\right] \quad (7)$$

and

$$f^{-}(t)=\frac{\varphi}{2\pi}+\sum_{n=1}^{+\infty}\left[\frac{2*(-1)^n}{n\pi}\cos(n\omega_T t-\frac{n\varphi}{2})\sin(\frac{n\varphi}{2})\right] \quad (8)$$

where φ is the phase shift angle, $0\le\varphi\le\pi$.

Assume the voltage drop across the filters is neglected. The output voltage appears at the primary side of the resonant tank is given by,

$$v_p(t)=v^{+}(t)f^{+}(t)+v^{-}(t)f^{-}(t) \quad (9)$$

Substituting (4), (5), (7) and (8) into (9) we get,

$$v_p(t)=\frac{3\sqrt{3}V_m}{\pi}\left\{\begin{array}{l}\left[1-\sum_{n=2,4,6\ldots}^{+\infty}\frac{2}{9n^2-1}\cos(3n\omega_0 t-\frac{n\pi}{2})\right]*\\ \left[\sum_{k=1,3,5\ldots}^{+\infty}\frac{2}{k\pi}\cos(k\omega_T t-\frac{k\varphi}{2})\sin(\frac{k\varphi}{2})\right]-\\ \left[\sum_{m=1,3,5\ldots}^{+\infty}\frac{2}{9m^2-1}\cos(3m\omega_0 t-\frac{m\pi}{2})\right]*\\ \left[\frac{\varphi}{2\pi}+\sum_{l=2,4,6\ldots}^{+\infty}\frac{2}{l\pi}\cos(l\omega_T t-\frac{l\varphi}{2})\sin(\frac{l\varphi}{2})\right]\end{array}\right\} \quad (10)$$

A simpler expression can be derived as follows by omitting the higher order harmonics in each expression (4), (5), (7) and (8).

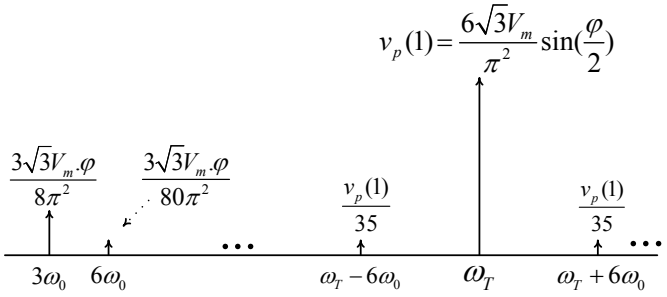

Fig. 4. FFT spectra of primary resonant tank voltage.

$$v_p(t)\approx\frac{6\sqrt{3}V_m}{\pi^2}\sin(\frac{\varphi}{2})\left\{\begin{array}{l}\cos(\omega_T t-\frac{\varphi}{2})+\\ \frac{1}{35}\cos\left[(\omega_T+6\omega_0)t-\frac{\varphi}{2}\right]+\\ \frac{1}{35}\cos\left[(\omega_T-6\omega_0)t-\frac{\varphi}{2}\right]\end{array}\right\}+$$
$$+\frac{3\sqrt{3}V_m.\varphi}{8\pi^2}\sin(3\omega_0 t) \quad (11)$$

Simplifying further we have,

$$v_p(t)\approx\frac{6\sqrt{3}V_m}{\pi^2}\sin(\frac{\varphi}{2})\cos(\omega_T t-\frac{\varphi}{2})+\frac{3\sqrt{3}V_m.\varphi}{8\pi^2}\sin(3\omega_0 t) \quad (12)$$

The FFT spectrum of this voltage is illustrated in Fig. 4. Since the other harmonic components of V_p are much less than the harmonic at the resonant angular frequency ω_T, $V_p(1)$, V_p can be considered to be an ideal sinusoidal voltage source for the primary resonant tank of IPT systems with the angular frequency ω_T.

III. Output Power and Efficiency Analysis of Series- Series Compensation Topology in IPT Systems

A. The load power analysis

The equivalent circuit of the topology presented in Fig. 2 is shown in Fig. 5.

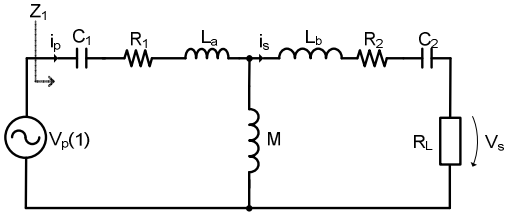

Fig. 5. The equivalent circuit of SS compensated IPT system of Fig. 2.

The equivalent load resistance R_L can be expressed in terms of DC load resistance as follows,

$$R_L=\frac{8}{\pi^2}R_T \quad (13)$$

where R_L is the equivalent load resistance referred to the resonant inductive side and R_T is the DC load resistance [5].

The equivalent circuit inductances are given by

$$\begin{aligned} L_a &= L_1 - M \\ L_b &= L_2 - M \end{aligned} \tag{14}$$

L_a and L_b are the leakage inductances of the primary and the pickup windings respectively and M is the mutual inductance of the windings.

It is obvious from Fig. 5 that the impedance referred to the voltage source side is given by,

$$Z_1 = \frac{M^2\omega^2}{j\omega\, L_2 - \dfrac{j}{\omega\, C_2} + R_2 + R_L} + j\omega L_1 - \frac{j}{\omega\, C_1} + R_1 \tag{15}$$

When IPT operates at the resonance angular frequency ω_T

$$Z_1(\omega_T) = \frac{M^2\omega_T^2}{R_2 + R_L} + R_1 \tag{16}$$

The current flow in the secondary winding at the angular frequency ω_T is given by,

$$|i_s| = \left| \frac{V_p(1)}{Z_1} \frac{j\omega_T M}{R_2 + R_L} \right| \tag{17}$$

The output power therefore is given by

$$\begin{aligned} P_{out} &= \frac{1}{2} R_L |i_{sm}|^2 \\ &= \frac{1}{2} R_L \frac{V_{pm}^2}{\left(\omega_T M + \dfrac{R_1(R_2 + R_L)}{\omega_T M} \right)^2} \\ &= P_{out}(R_L, M) \end{aligned} \tag{18}$$

where V_{pm} is the amplitude voltage of $V_p(1)$.

The output load power is a function of mutual inductance M and load resistance R_L.

The mutual inductance is a function of the coupling coefficient k which depends on the distance between the two winding coils and is expressed as follows,

$$M = k\sqrt{L_1 L_2} \tag{19}$$

The maximum load power transferred can be determined by choosing the mutual inductance or load resistance satisfy the following expressions,

$$\frac{dP}{dM} = 0 \quad \text{(20a)} \quad \text{or} \quad \frac{dP}{dR_L} = 0 \quad \text{(20b)}$$

From (20a),

$$P_{out\_Max}\Big|_{R_L = const} = \frac{1}{8} \frac{R_L}{R_1(R_2 + R_L)} V_{pm}^2 \tag{21a}$$

$$M\Big|_{P_{out}Max} = \frac{\sqrt{R_1(R_2 + R_L)}}{\omega_T} \tag{21b}$$

From (20b),

$$P_{out\_Max}\Big|_{M = const} = \frac{V_{pm}^2}{4F} \tag{22a}$$

where

$$F = R_1 + \frac{R_1^2 R_2}{(\omega_T M)^2} + \frac{R_1^2}{(\omega_T M)^2} \sqrt{R_2^2 + \frac{2R_2}{R_1}(\omega_T M)^2 + \frac{(\omega_T M)^4}{R_1^2}}$$

$$R_L\Big|_{P_{out}Max} = \sqrt{R_2^2 + \frac{2R_2}{R_1}(\omega_T M)^2 + \frac{(\omega_T M)^4}{R_1^2}} \tag{22b}$$

B. The efficiency analysis

Assume that the power losses of the converters can be neglected, the efficiency of IPT systems with SS topology presented in Fig. 5 is given by,

$$\begin{aligned} \eta &= \frac{|i_L|^2 R_L}{|i_L|^2 R_L + |i_p|^2 R_1 + |i_s|^2 R_2} \\ &= \frac{1}{1 + \dfrac{R_2}{R_L} + \dfrac{R_1}{R_L}\left(\dfrac{R_2 + R_L}{\omega_T M} \right)^2} = f(R_L, M) \end{aligned} \tag{23}$$

It is obvious that the efficiency is proportional to the mutual inductance, i.e. the higher the mutual inductance, the higher the efficiency. In another words, the increase in distance between two windings coils makes the efficiency smaller. As η is also a function of R_L it can be maximized by tuning the load resistance.

By using,

$$\frac{d\eta}{dR_L} = 0 \tag{24}$$

Maximum efficiency can be determined as follows,

$$\eta_{\max} = \frac{1}{1 + \dfrac{2R_1R_2}{(\omega_T M)^2} + \dfrac{2R_1}{(\omega_T M)^2} \sqrt{R_2^2 + \dfrac{R_2}{R_1}(\omega_T M)^2}} \tag{25}$$

And

$$R_L\big|_{\eta=\eta_{MAX}} = \sqrt{R_2^2 + \frac{R_2}{R_1}(\omega_T M)^2} \quad (26)$$

Actually, we cannot tune the load resistance in almost of applications. However, if we know the range of the load resistance, we can design an IPT system with appropriate parameters for maximizing the system efficiency or output power load. In these cases, the analysis (13)-(26) will be useful.

IV. SIMULATION RESULTS

In the previous section, the proposed IPT system has been mathematically modeled. This section will present some simulation results to verify the viability of the proposed concept. The parameters of the simulation are given in Table 1. Figs. 6,7 and 8 present the simulation results in the case of phase shift angle $\varphi = \pi$ while Figs. 9,10 and 11 present the simulation results in case of phase shift angle $\varphi = \pi/2$. R_L is designed for maximizing the system efficiency: $R_L = 2.64\ \Omega$ ($R_T = 3.258\ \Omega$) in all of these results. Fig. 12 presents the output power in the case of R_L is designed for maximizing the output power: $R_L = 69.74\ \Omega$ ($R_T = 86\ \Omega$).

Table 1. Parameters for simulation

Parameters	Symbols	Value	Unit
Input phase voltages (RMS)	v_a, v_b, v_c	50	V
Input frequency	f_o	50	Hz
Primary and secondary inductance	$L_1 = L_2$	280	μH
Primary and secondary resistance	$R_1 = R_2$	0.1	Ω
Primary and secondary compensated capacitance	$C_1 = C_2$	0.1	μF
Switching frequency	f_T	30	kHz
Coupling coefficient	k	0.05	

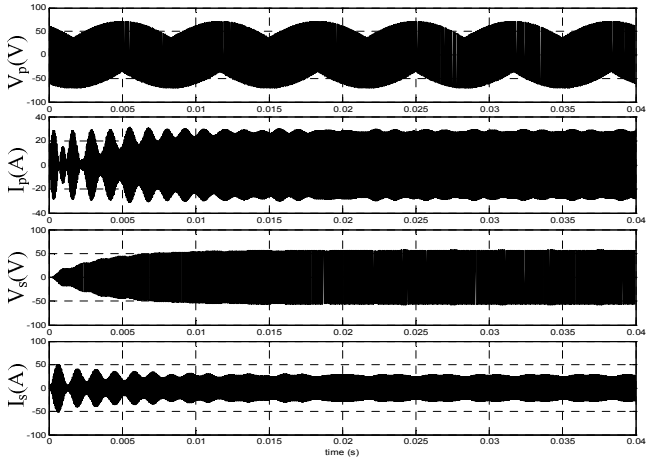

Fig. 6. Primary and pick up voltages and currents when phase shift angle $\varphi = \pi$.

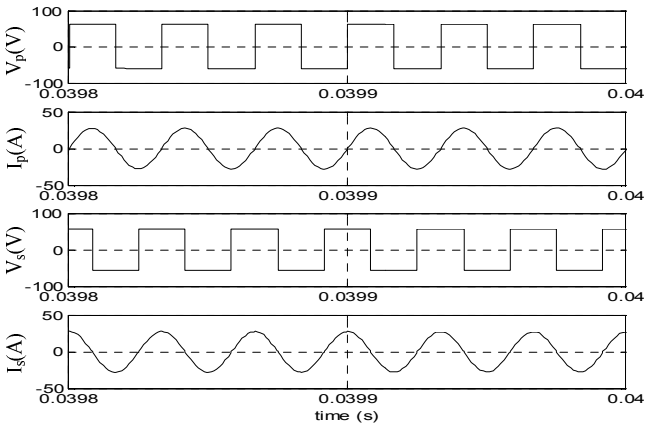

Fig. 7. Instantaneous voltages and currents from primary and pickup sides when shift angle $\varphi = \pi$.

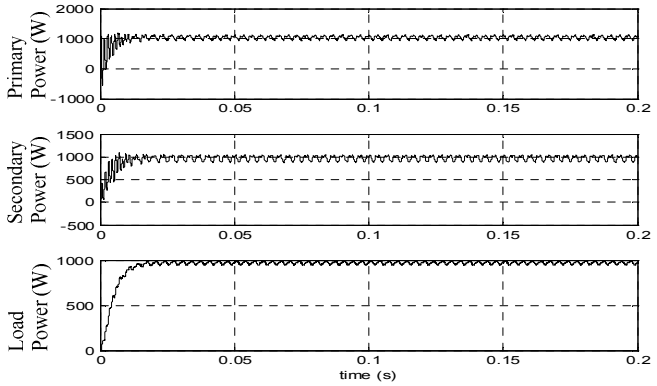

Fig. 8. Input and output power of the system when R_L is designed for maximizing the efficiency and $\varphi = \pi$.

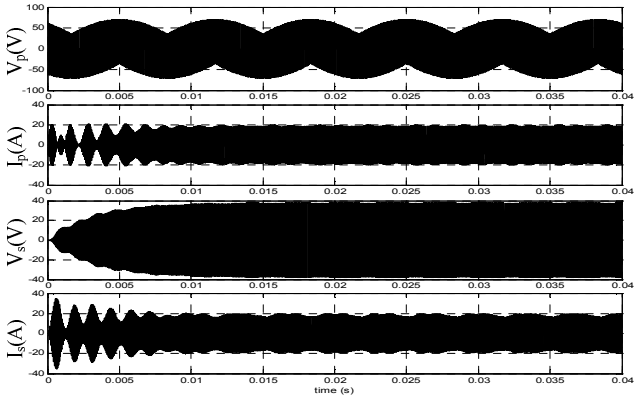

Fig. 9. Primary and pick up voltages and currents when phase shift angle $\varphi = \pi/2$.

It can be seen from Figs. 7 and 10 that the primary and the pickup currents are sinusoidal at the resonant frequency. Figs. 8 and 11 present the primary, secondary and load power of the proposed system with the maximum efficiency is about 93%. Furthermore, it can be seen that the output power can be controlled by phase shift angle φ. The load power shown in Figs. 8 and 11 are about 980 W and 470 W with the phase shift angles of $\varphi = \pi$ and $\varphi = \pi/2$ respectively.

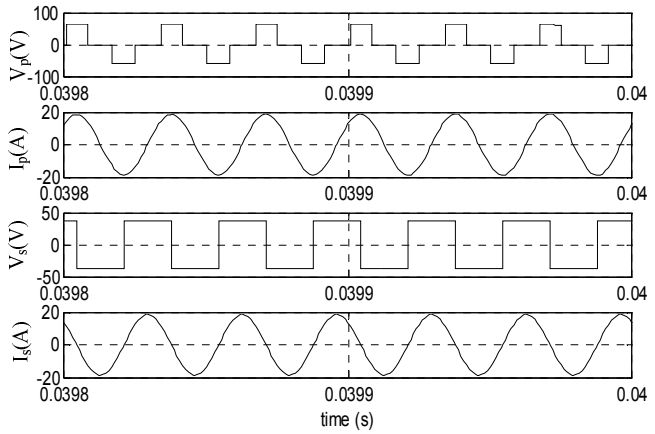

Fig. 10. Instantaneous voltages and currents from primary and pickup sides when phase shift angle $\varphi = \pi/2$.

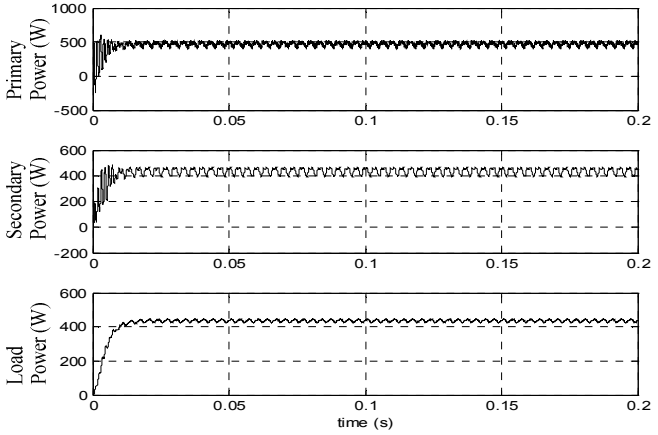

Fig. 11. Input and output power of the system when R_L is designed for maximizing efficiency and $\varphi = \pi/2$.

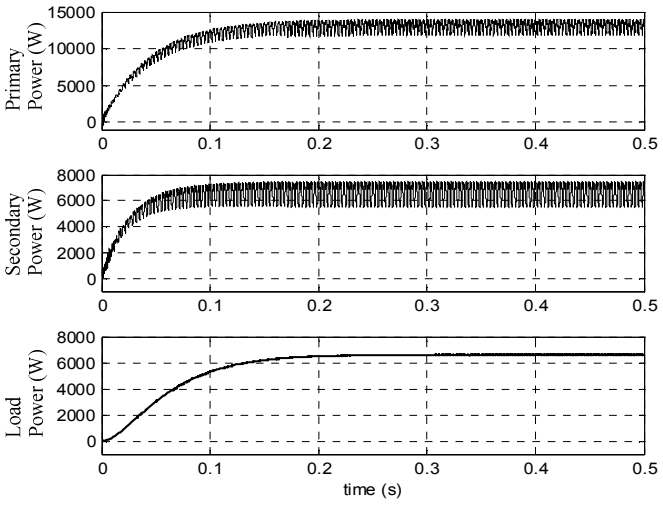

Fig. 12. Input and output power of IPT system when R_L is designed for maximizing output power and $\varphi = \pi$.

The maximum output power of 6.8 kW seen in Fig. 12 is compatible with the value calculated using 22(a) and it has been transferred through the air gap with an efficiency of about 50%.

V. CONCLUSIONS

A matrix converter based IPT system has been proposed to improve the overall efficiency of system through the reduction of power conversion stages. A series compensated IPT system has directly been excited from the supply mains to generate a high frequency current in the resonant tank. A mathematical model for the proposed system has also been presented with simulated results to demonstrate the feasibility of the proposed topology. With less number of conversion stages, the matrix converter based IPT topology is expected to be efficient, low in cost and suitable for high power applications.

REFERENCES

[1] Madawala, U.K.; Thrimawithana, D.J. "A Bidirectional Inductive Power Interface for Electric Vehicles in V2G Systems". *IEEE Trans. On Ind. Elect.,* Vol. 58, No. 10, Oct. 2011, pp. 4789 – 4796.

[2] Thrimawithana, D.J.; Madawala, U.K.; Yu Shi. "Design of a bi-directional inverter for a wireless V2G system". IEEE International Conference on Sustainable Energy Technologies (ICSET), 2010 .

[3] D. J. Thrimawithana and U. K. Madawala. "A novel matrix converter based bi-directional IPT power interface for V2G applications", IEEE Inter. Energy Conf. and Exhibition, 2010.

[4] G. A. Covic, J. T. Boys, M. L. G. Kissin, and H. G. Lu. "A three-phase inductive power transfer system for roadway powered vehicles". *IEEE Trans. on Ind. Elect.,* Vol. 54 , Iss.6. 2007. Pp.3370 – 3378.

[5] Hao Leo Li. "High Frequency Power Converters Based on Energy Injection Control for IPT Systems". PhD Thesis, Depart. of Electrical and Electronic Engineering The Uni. of Auckland. Jan. 2011.

[6] Aiguo Patrick Hu. "Selected Resonant Converters For IPT Power Supplies". PhD Thesis, Depart. of Electrical and Electronic Engineering The Uni. of Auckland. Oct. 2001.

[7] Si, P.; Hu, A.P.; Hsu, J.W.; Chiang, M.; Wang, Y.; Malpas, S.; Budgett, D. "Wireless Power Supply for Implantable Biomedical Device Based on Primary Input Voltage Regulation". IEEE Conference on Ind. Elect. and Appl., 2007. Pp. 235 – 239.

[8] A. Alesina and M. G. B. Venturini, "Analysis and design of optimum-amplitude nine-switch direct AC-AC converters," *IEEE Trans. on Power Electronics*, vol. 4, no. 1, pp. 101-112, January 1989.

[9] A. Ecklebe, A. Lindemann and S. Schulz. "Bidirectional switch commutation for a matrix converter supplying a series resonant load", *IEEE Trans. Power Electron.*, vol.24, no.5,2009. pp.1173 -1181.

[10] A. Ecklebe and A. Lindemann. "Bi-directional Switch Commutation for a Resonant Matrix Converter supplying a Contactless Energy Transmission System". Power Conversion Conference - Nagoya, 2007. pp. 792-799.

[11] Kurschner, D.; Mecke, R. "Matrix converter with advanced control for contactless energy transmission". European Conference on Power Electronics and Applications, 2007.

[12] H.L. Li, Hu. A.P., Covic. G.A., "A Direct AC–AC Converter for Inductive Power-Transfer Systems". *IEEE Trans on Pow. Elect*. Vol.27, No.2, Feb.2012.

[13] Seung-Hwan Lee; Lorenz, R.D. "Development and Validation of Model for 95%-Efficiency 220-W Wireless Power Transfer Over a 30-cm Air Gap". *IEEE Trans. Ind. Appl.*. Vol.47, No.6, Nov.2011.

[14] John I. Rodriguez , and Steven B. Leeb. "A Multilevel Inverter Topology for Inductively Coupled Power Transfer". *IEEE Trans. On Pow. Elect.,* Vol. 21, No. 6, Nov. 2006. Pp.1607- 1617.

[15] Trentin, A.; Zanchetta, P.; Clare, J.; Wheeler, P. "Automated Optimal Design of Input Filters for Direct AC/AC Matrix Converters". *IEEE Trans. on Ind. Elect.,* Vol. 59 , Iss.7. 2012. Pp. 2811 – 2823.

[16] Yakovlev, A.; Sanghoek Kim; Poon, A. "Implantable biomedical devices: Wireless powering and communication". *Communications Magazine, IEEE.* Vol.50, Iss. 4, 2012. Pp.152 – 159.